N73-25421
NASA CR-2271

NASA CONTRACTOR REPORT

NASA CR-2271

INVESTIGATION OF ATOMIC OXYGEN-SURFACE INTERACTIONS RELATED TO MEASUREMENTS WITH DUAL AIR DENSITY EXPLORER SATELLITES

by Bernard J. Wood, C. M. Ablow, and Henry Wise

Prepared by
STANFORD RESEARCH INSTITUTE
Menlo Park, Calif. 94025
for Langley Research Center

NATIONAL AERONAUTICS AND SPACE ADMINISTRATION • WASHINGTON, D. C. • JUNE 1973

1. Report No.	2. Government Accession No.	3. Recipient's Catalog No.
NASA CR-2271		

4. Title and Subtitle	5. Report Date
INVESTIGATION OF ATOMIC OXYGEN-SURFACE INTERACTIONS RELATED TO MEASUREMENTS WITH DUAL AIR DENSITY EXPLORER SATELLITES	June 1973
	6. Performing Organization Code
7. Author(s)	8. Performing Organization Report No.
Bernard J. Wood, C. M. Ablow, and Henry Wise	
	10. Work Unit No.
9. Performing Organization Name and Address	863-11-00-01-00
Stanford Research Institute	11. Contract or Grant No.
333 Ravenswood Avenue	NAS1-10962
Menlo Park, CA 94025	13. Type of Report and Period Covered
12. Sponsoring Agency Name and Address	Contractor Report
National Aeronautics and Space Administration	14. Sponsoring Agency Code
Washington, DC 20546	

15. Supplementary Notes

16. Abstract

For a number of candidate materials of construction for the Dual Air Density Explorer Satellites the rate of oxygen atom loss by adsorption, surface reaction, and recombination was determined as a function of surface treatment and temperature. Plain aluminum and anodized aluminum surfaces exhibit a collisional atom loss probability $\alpha < 10^{-2}$ in the temperature range 140 - 360°K, and an initial sticking probability $S_o < 10^{-2}$. For SiO_x - coated aluminum in the same temperature range, $\alpha < 10^{-3}$ and $S_o < 10^{-3}$. Atom-loss on gold is relatively rapid ($\alpha > 10^{-2}$). S_o for gold varies between 0.25 and unity in the temperature range 360 - 140°K.

17. Key Words (Suggested by Author(s))	18. Distribution Statement
Atoms; Atomic Oxygen Surface; Recombination; Adsorption Satellite; Gas-Surface Reaction	Unclassified - Unlimited

19. Security Classif. (of this report)	20. Security Classif. (of this page)	21. No. of Pages	22. Price*
Unclassified	Unclassified	53	$3.00

*For sale by the National Technical Information Service, Springfield, Virginia 22151

LIST OF SYMBOLS

A	area
a	semi-major axis of elliptical orbit
B b	surface atom loss parameters (page B-3)
D	diameter of satellite
e	eccentricity of orbit
F	conductance
f	atom flux or (1-h)
h	hole fraction of satellite surface
K	surface reaction rate parameter
k	rate constant
n	particle number density (volumetric or surface, as indicated by subscript)
P	pressure
p	(1-h)/h
Q	mass flow rate
R	radius of satellite
r	distance from center of earth
S	sticking probability
T	satellite period
t	time
V	fv/v_g
v	velocity
Z	surface collision flux
α	loss coefficient
β	angle of satellite in orbit
γ	atom recombination probability
φ	phase lag
σ	collision number (Eq. 2)
θ	fractional surface coverage

Superscript:

*	value of parameter with no specimen in reactor

Subscripts:

A	ambient value
a	steady state value
e	reactor exit
g	gaseous species
i	reactor inlet
O	oxygen atoms
o	initial value
max	maximum value
R	reactor
s	specimen surface
1	adsorption
2	adatom-adatom recombination
3	gasatom-adatom recombination

INVESTIGATION OF ATOMIC OXYGEN-SURFACE INTERACTIONS RELATED TO MEASUREMENTS WITH DUAL AIR DENSITY EXPLORER SATELLITES

Bernard J. Wood, C. M. Ablow, and Henry Wise
Stanford Research Institute
Menlo Park, California 94025

INTRODUCTION AND OBJECTIVE

The problem of quantitative evaluation of the atomic oxygen concentration in the earth's upper atmosphere from data reported by satellite-borne mass spectrometers has been amply documented by a number of independent investigators (ref. 1). To relate the actual atom number density in the space vehicle's environment to that recorded by the onboard mass spectrometer, one needs detailed information on the loss of oxygen atoms due to their interaction with solid surfaces, including adsorption, chemical reaction, and catalytic production of molecular oxygen.

In the Dual Air Density Explorer satellites, currently being planned, sampled gases will come into contact with large surface areas of metal. The geometry of each satellite is such that oxygen atoms will have the opportunity for multiple collisions with the metal surfaces before passing through the ion source of a mass spectrometer. Consequently it is of importance to evaluate quantitatively the rate of loss of oxygen atoms by adsorption and recombination on metal surfaces of interest under conditions of oxygen pressure and surface temperature similar to those anticipated in the upper atmosphere.

The objective of this project was to examine quantitatively the rate and mechanism of oxygen atom loss on candidate materials of construction for the Dual Air Density Explorer satellites as a function of material, surface treatment, and temperature.

EXPERIMENTAL APPROACH

Measurement of Total Atom Loss Rates

In our studies of the probability of atom loss due to surface interaction we employ a glass reaction vessel in which the entering flux of oxygen atoms is held constant. Change in the mass fraction of gaseous atoms that pass through the vessel is negligibly small, due to the inert character of the glass wall. The mass flow rate of atoms at the outlet of the vessel Q^* is measured with a mass spectrometer. We evaluate the overall rate of atom loss on a metal surface by observing the reduced mass flow rate of atoms Q that occurs when a specimen of the metal of interest is inserted into the reactor.

Under the conditions of free molecular flow that apply throughout the pressure range employed in our experiments, simple kinetic theory suggests that once an atom enters the reactor it will depart through the outlet or the inlet after suffering multiple collisions with the surface. However, if the atom adsorbs or recombines on the surface during one of these collisions, it will remain in the reactor or leave as a molecule. A detailed model has been developed (ref. 2) that describes the variation in atom flux within a cylindrical reactor containing reactive surfaces. Computations with this model suggest that, for surfaces with modest reactivity, the exit flux of oxygen atoms may be reasonably approximated by a simple analysis in which the rate at which atoms enter the reactor is balanced by the loss of atoms on the reactive surface and their departure through the inlet or outlet. Hence, the average atom flux f in the reactor is given by the equation:

$$f = \frac{f_o A_i}{A_i + A_e + \alpha A_s} \qquad (1)$$

in which f_o is the atom flux entering the reactor; A is the area identified by the subscripts i for inlet, e for exit and s for specimen; and α, termed the loss coefficient, represents the probability that a colliding atom will stick or recombine on the specimen surface. It is assumed (and has been experimentally justified, p. 9) that steady state loss of oxygen atoms on the reactor wall is negligibly small. The total mass flow rate through the reactor outlet Q is given by the product fA_e, so that in the presence of a reactive specimen $fA_e \equiv Q = f_o A_i A_e / [A_i + A_e + \alpha A_s]$, and in the absence of a reactive surface ($\alpha A_s = 0$), $f^* A_e \equiv Q^* = f_o A_i A_e / [A_i + A_e]$. Thus,

$$\frac{Q}{Q^*} = \frac{A_i + A_e}{A_i + A_e + \alpha A_s}$$

or

$$\frac{Q}{Q^*} = \frac{1}{1 + [\alpha A_s / (A_i + A_e)]} = \frac{1}{1 + \alpha\sigma} \qquad (2)$$

where σ can be shown to represent the collision number of the reactor, or the average number of collisions an atom will make on the surface during its sojourn in the reactor. By means of Eq. (2), we evaluate α from measured values of Q/Q^*.

Specific Pathways for Atom Loss

The entering mass flow rate of atoms into the reactor is maintained constant. The metal specimen can be raised to an elevated temperature in order to rapidly desorb any reversibly adsorbed oxygen, so that the kinetics of adsorption and desorption of oxygen can be measured. The specimen is heated by passage of an electric current, and the oxygen that desorbs from the surface causes an increase in the mass flow rate of

molecular oxygen through the reactor outlet:

$$Q_{O_2} = Q_a + \dot{n}_s A_s/2 \tag{3}$$

where A_s is the total area of the test specimen, $\dot{n}_s$ is the rate of desorption of oxygen from the specimen surface and the subscript a represents steady-state flow prior to specimen heating. By integrating Eq. (3) over the period of heating time t required to desorb all oxygen, we obtain an expression for the mass of gas n_s on the specimen surface prior to heating:

$$n_s = 2(Q_{O_2} - Q_a)t/A_s \tag{4}$$

We evaluate the rate of adsorption of oxygen by measuring n_s following exposure of the specimen to a fixed atomic oxygen flux for successively different periods of time.

We can envision three possible pathways by which oxygen atoms can reversibly interact with a metal surface:

adsorption:	$O(g) + (s) \rightarrow O(s)$	$\dot{n}_s = S_o v_g n_g (1-\theta)/4$
recombination: (adatom-adatom)	$O(s) + O(s) \rightarrow O_2(g) + 2(s)$	$\dot{n}_s = k_2 n_s^2$
recombination: (gasatom-adatom)	$O(g) + O(s) \rightarrow O_2(g) + (s)$	$\dot{n}_s = k_3 n_s n_g$

where O(g) and O(s) refer to gaseous and adsorbed atomic oxygen, respectively, $O_2(g)$ represents gaseous molecular oxygen, (s) refers to an available surface, S_o is the initial sticking coefficient for adsorption, the k_2 and k_3 are rate constants for adatom-adatom and gasatom-adatom recombination, respectively, n_s is the number of sorption sites per unit area, $\dot{n}_s$ is the time rate of change of sorbed atomic oxygen per unit

area, θ is the fractional coverage ($n_s/n_{s\,max}$), n_g is the number density of gaseous atomic oxygen, and v_g is the average atomic speed.

(If the metal forms a heat-labile oxide, another equation would have to be included in this scheme. The amount of molecular oxygen which chemisorbed on the materials used in our experiments was at the lower limit of detectability. Hence, we may disregard the reverse of the above recombination equations as a mechanism for supply of adatoms to the surface. Also, due to energy considerations, the reverse of the adsorption reaction may be disregarded.)

At any moment the net rate of accumulation of atoms on the surface is determined by the dynamic balance between these three processes, thus,

$$\dot{n}_s = S_o n_g v_g (1-\theta)/4 - k_2 n_s^2 - k_3 n_s n_g \qquad (5)$$

It is of interest to examine Eq. (5) under special conditions.

1) When $\theta = 0$, $\dot{n}_s = S_o n_g v_g/4$. Consequently, if we measure the initial adsorption rate $\dot{n}_{so}$ on a clean surface in a known partial pressure of atomic oxygen, we may evaluate the sticking coefficient S_o defined as the ratio of adsorption rate over collision rate Z. From kinetic theory $Z = n_g v_g/4$. Therefore

$$S_o = \dot{n}_{so}/Z \qquad (6)$$

2) When $n_g = 0$, but $n_s > 0$, $\dot{n}_s = k_2 n_s^2$. Hence, from a measurement of the initial rate of desorption of oxygen from a surface with known initial coverage n_{so} , we may evaluate k_2 .

3) When $\dot{n}_s = 0$, that is, at steady state, $S_o n_g v_g (1-\theta)/4 = k_2 n_s^2 + k_3 n_s n_g$. Hence, by measurement of n_s and n_g at steady state, and by use of values of S_o and k_2 obtained under other conditions, we may evaluate k_3 .

From the experimental study of the overall atom loss, the values of α determined at steady state represent the global loss rate of atoms on the specimen, given by $\dot{n} = \alpha Z$. For an atom removal rate $\dot{n}$ of first order with respect to atomic oxygen, $\dot{n} = k_\alpha n_g n_s$. Thus a value of k_α may be computed from the measured values of α and n_s at steady state:

$$k_\alpha = \alpha v_g / 4 n_s \quad . \tag{7}$$

Although k_α is not used to determine S_o, k_2, and k_3, it does describe the overall atom loss coefficient of the specimen surface.

In summary, from our measurements of n_s and $\dot{n}_s$, and from values of n_g derived from the mass spectrometer data, we are able to determine the rate constant for each pathway by which oxygen atoms can interact with the metal surface.

Page Intentionally Left Blank

EXPERIMENTAL DETAILS

Apparatus Geometry

Two separate reactors were employed in this study. Both were constructed of Pyrex glass. In the first (Fig. 1a), which was employed also in an earlier study (ref. 3), all components shared a common axis of cylindrical symmetry. In the second (Figs. 1b and 2) the atom source and the mass spectrometer were each turned through 90° so that they were not in line-of-sight of the specimen in the reactor. In both cases foil specimens in the form of long, narrow ribbons (Fig. 3) were suspended from electrical leadthroughs at the upper (outlet) end of the reactor. In reactor "b" (Figs. 1 and 2) the leadthroughs were 1/4 inch copper rods which could be cooled by inundation with liquid nitrogen. The large copper rods provided an efficient heat transfer path which permitted the lowest portion of the specimen to reach temperatures as low as 140° K within 10 minutes of the commencement of cooling.

Each part of each apparatus was cylindrical in shape. Consequently the vacuum conductance F for each section could be calculated from the established formula for molecular flow of oxygen through short pipes, and the reciprocal of the overall conductance could be reliably estimated by summing the reciprocals of the individual conductances (ref. 4). The dimensions and the conductances of the two pieces of apparatus are given in Table 1.

Generation of Oxygen Atoms

Atomic oxygen is formed by thermal dissociation of molecular oxygen on a tungsten surface. The rate of dissociation of oxygen at subatmospheric pressures on heated tungsten surfaces has been studied in detail

by Schissel and Trulson (ref. 5). On the basis of their data we chose to operate our tungsten ribbon in the temperature range 2150-2250°K, where tungsten oxide formation is negligibly small, CO production is within reason, and the atomic oxygen flux is satisfactory.

Of course even in a reactor with completely inert surfaces, the steady-state absolute flux of atoms at the outlet must be less than that at the inlet by the factor representative of the net transmission probability of the reactor and its apertures. Values of transmission probability for our apparatus were computed from the data of Berman (ref. 6) for cylindrical tubes. We used these values to predict the atom flow rate at the outlet of the empty reactor from the kinetic data of Schissel and Trulson. (We assumed in this calculation that only the atoms generated on the central 0.02-cm^2 region of the tungsten ribbon have access to the reactor. This area represents the area of a thin-edge aperture with the conductance of the reactor inlet and thus approximates the clear view of the reactor interior from the tungsten surface.) A comparison of the calculated atom flow rates with those observed is given in Table 2. In nearly all cases, the observed values of atom flow rate exceed those predicted. In view of the approximate nature of (1) the estimated reactor inlet view area of the tungsten ribbon, and (2) the inlet conductance, the experimental results suggest there is a negligibly small atom loss on the Pyrex wall of the reactor. These observations are in agreement with reported (ref. 7) low values of catalytic activity of glass and quartz for oxygen atom recombination ($\gamma \tilde{=} 10^{-4}$; i.e., only one out of 10^4 collisions results in atom loss by recombination).

Mass Spectrometer Calibration

The geometry of the experimental arrangement is such that the quadrupole mass spectrometer observes the effective mass flow rate of species emerging from the reactor outlet. The mass specrometer was

calibrated for molecular oxygen by computing the net mass flow of gas Q_{O_2} through the apparatus from the observed pressure difference between the two identical ion gauges (P_S and P_A in Fig. 1) and the net conductance of the apparatus between the gauges (Table 1):

$$Q_{O_2} = F_{net} (P_S - P_A) \quad .$$

In the range $10^{-6} < Q_{O_2} < 10^{-3}$ torr-ℓ/sec, the mass spectrometer signal was found to be proportional to Q_{O_2} .

The mass spectrometer was calibrated after each experiment to allow corrections for variation in electron multiplier sensitivity. An electron energy of 50 V was employed in the ion source of the mass spectrometer. At this energy, the reported (ref. 8) ionization cross sections for O, O_2, and CO are comparable, hence we assume a common calibration constant for all the major gases observed in our apparatus.

In addition we determined the cracking pattern of H_2O, CO, CO_2, and O_2 , all of which contribute to the mass spectrometer signal at AMU 16. All of the values of Q_{16} reported in this document have been corrected for the contributions of these other components according to the cracking patterns given in Appendix A.

Estimation of n_g in Reactor

We had no direct measurement of gaseous pressure in the reactor, hence we estimated both P_O and P_{O_2} from the mass spectrometer data and the apparatus geometry. Based on the various evidences cited above, we could assume that the steady-state mass ratio of atomic oxygen to molecular oxygen was uniform throughout the empty reactor. Hence the value of $\left(I^+_{16} / I^+_{32}\right)_E$ measured at the empty reactor outlet would be identical with the value of this ratio at the reactor inlet. When a specimen was in the reactor, however, $\left(I^+_{16} / I^+_{32}\right)_S$ observed at the outlet would

have a lower value than that at the inlet. The pressure of molecular oxygen at any point in the system would be relatively unchanged in the two cases, since it comprised more than 90% of the gaseous mass in the reactor. We therefore calculated the pressure of O_2 at the exit end and the inlet end of the reactor from the measured pressure P_A at the mass spectrometer, the mass flow rate Q, and the conductances of the outlet F_e and of the reactor F_R :

$$P_{O_2} \text{ exit} = (Q/F_e) + P_A$$

$$P_{O_2} \text{ inlet} = (Q/F_R) + P_{O_2} \text{ exit}$$

Then, from the measured values of $\left(I^+_{16}/I^+_{32}\right)$:

$$P_O \text{ exit} = P_{O_2} \text{ exit} \left(I^+_{16}/I^+_{32}\right) S$$

$$P_O \text{ inlet} = P_{O_2} \text{ inlet} \left(I^+_{16}/I^+_{32}\right) E$$

The oxygen-atom pressure in the reactor employed in our computations is taken as the arithmetical mean between these two values of P_O .

Specimens

In the course of this study, we examined a variety of plain aluminum and modified aluminum surfaces, in addition to a pure gold foil.

The aluminum and vapor deposited gold-on-aluminum specimens were supplied by Langley Research Center. They were identified as follows:

No. 6: 1235-0 aluminum, plain, 0.005 in. thick

No. 14: 1235-0 aluminum, 0.005 in. thick, 3500 Å gold on both sides

No. 16: 1235-0 aluminum, plain, 0.005 in. thick freon cleaned.

The anodized aluminum specimen was kindly provided by Mr. Richard Smith of the Kaiser Center for Technology in Pleasanton, California. He deposited an approximately 0.0001-in.-thick anodic coating on a piece of the Langley No. 16 aluminum in a 15 wt % sulfuric acid electrolyte at 297°K with a current density of 12 amp/ft^2. The specimen was subsequently washed in flowing, distilled water for 3 hrs but was not "sealed" in boiling water.

The SiO_x coatings were sputtered on both sides of specimens cut from Langley No. 16 aluminum by Mr. William Cornelius of SRI's Electromagnetic Techniques Laboratory. The thickness of the SiO_x layer is in the range 600-1000 Å.

The gold specimen is the identical 0.002-in.-thick gold foil strip employed in our earlier study (ref. 3). It is reported to be 99.99% pure.

Specimens of an aluminum-mylar laminate, overcoated with SiO_x, were also supplied by Langley Research Center. These specimens continuously outgassed large quantities of organic vapors under the vacuum and surface conditions prevailing in our reactor ($P_{background} \approx 10^{-8}$ torr, surface temperature 360°K) due probably to the elevated temperature. Consequently we were unable to carry out quantitative measurements of oxygen atom interaction rates on this material.

Specimen Pretreatment

A specimen of each material was examined initially for oxygen atom interaction without any pretreatment. The specimens were cut with a clean (degreased) razor blade and were handled with white gloves during insertion into the reactor. Typically, a specimen was mounted in the reactor on one day and the system was pumped down during the night in preparation for experimental measurements on the following day. During this pumpdown period, the pressure in the system diminished from 10^{-6} to

10^{-8} torr. Water was the major contaminant remaining in the system after this procedure. Base pressures in the system could be reduced to near 10^{-9} torr by an overnight bakeout at 550°K. This treatment reduced the residual pressure of H_2O by a factor of ten while it simultaneously subjected the specimen to a gentle vacuum anneal. (Bakeout of the system did not appear to affect the observed mass flow rates of atomic oxygen from the empty reactor.)

The specimens could be vacuum annealed also by resistance heating. A current of 12 amp was passed through the 0.005-in.-thick aluminum specimens that were annealed in this manner. This raised the specimen temperature (as measured by a thermocouple attached to the midpoint of representative specimens) to 480°K in a glass vacuum chamber (equivalent to reactor "a") and to 590°K in reactor "b" (See Fig. 1). The difference in attained temperature of an identical specimen in the two environments was attributed to the bright stainless steel tube surrounding reactor b, which served as a radiation shield and thermal insulator. In consequence of this shielding, the steady-state temperature of a specimen under examination in reactor "b", heated indirectly by the tungsten atom source, was measured to be 360°K. The steady-state surface temperature of a specimen in reactor "a" was estimated to be 330°K, based on the observed temperature rise of a heated specimen in a glass vacuum bottle. (Direct temperature measurements of specimens in reactor "a" could not be made due to the lack of a provision for insertion of a thermocouple in the vacuum system.)

Atom loss rates were evaluated also on specimens which were heated in the presence of atomic oxygen. In these cases, a 12-amp heating current was employed for a duration of ten minutes or less.

The specimens were exposed to atomic oxygen for periods of 1 to 2 hrs during a typical experiment. Long duration exposures were not

carried out because the lifetime of the tungsten ribbon atom source was limited to approximately 15 hrs.

The gold foil specimen was vacuum annealed for several minutes at 890°K preceding each experiment. In this case, the surface temperature was measured in reactor "a" with a radiation thermomenter (Huggins infrascope). The 9-amp current required to attain this temperature in reactor "a' undoubtedly raised the surface temperature to approximately 1000°K when the specimen was annealed in reactor "b".

Page Intentionally Left Blank

EXPERIMENTAL RESULTS

The mass flow rate of atomic oxygen through the reactor outlet was determined from the mass spectrometer-measured values of Q_{O_2} and the ratio of ion currents for AMU16 and AMU32, I_{16}^+/I_{32}^+ (I_{16}^+ corrected for cracking of other components). Data were collected for each specimen and with the empty reactor over the range $10^{-6} < Q_{O_2} < 10^{-4}$ torr-ℓ/sec. Data from typical experiments are shown in Figure 4. All of the loss rate data obtained with various specimens in steady-state experiments are summarized in Table 3. Mean values of Q/Q^* from all experimental points are shown with their respective standard deviations. From this data, the mean values of loss coefficient α were computed, in addition to the values of α_{max} based in each case on the statistically lowest values of Q/Q^*.

In all experiments carried out at ambient temperature or higher, the flow rates of three impurities, H_2O, CO, and CO_2, were comparable in magnitude to the flow rate of oxygen atoms. In the subambient temperature experiments, however, the observed flow rate of H_2O was substantially reduced.

Experimental adsorption/desorption curves for various surfaces at ambient temperature are shown in Figures 5 through 10. Initial slopes were taken from the best-fit curves drawn through the data points. The rate constants calculated from these data are summarized in Table 4. A value of $n_{s\ max} = 1.1 \times 10^{15}$ atoms/cm^2 was assumed for these calculations. This number of available sites is representative of an atomically smooth metal crystal of random orientation. Macroscopic roughness would increase the value of this parameter possibly by as much as a factor of two. On a nonelemental crystal, lattice atoms of different size and chemical nature make up the surface. As a result, the effective number of available sites might be considerably less than 1.1×10^{15} cm^{-2}.

Page Intentionally Left Blank

DISCUSSION

The basic overall atom loss rate data, summarized in Table 3, indicate that significant variations in loss coefficient α exist between different surfaces and between identical surfaces subjected to various pretreatments. However, the absolute value of α for any surface does not exceed 2×10^{-2} under our steady-state conditions ($3 \times 10^{8} < n_g < 6 \times 10^{9}$ atoms/cm^3). Thus, based on Eq. (2), in a vessel with $\sigma = 100$, the fraction of incoming atoms lost would not exceed 0.7 for the most active material.

It is important to note that the lowest value of atomic oxygen number density employed in our experiments will be comparable to the highest ambient value to be experienced by the Dual Air Density lower satellite. Consequently, one must consider the probability that the coverage of adsorbed oxygen on the satellite surface may be substantially lower than the saturation values observed in our experiments. The atomic oxygen adsorption rate on the bare surface, evaluated in our experiments, may be used to estimate the upper limit of atom loss for the low values of coverage. Examination of the values of S_o in Table 4 shows that a sparsely covered gold surface would exhibit a considerably greater atom loss rate than either of the aluminum surfaces or the SiO_x surface.

The aluminum specimens exhibit some changes in activity related to their pretreatment (see Table 3). The untreated plain aluminum and anodized aluminum specimens gave consistently low values of α at 330°K. Vacuum annealing of these materials produced surfaces with somewhat higher activity (greater values of α), while heating the specimens in

the presence of atomic oxygen increased the activity still further. During annealing, H_2O was observed to be the major component desorbed from the aluminum surfaces. Exposure of an annealed, anodized aluminum specimen to water vapor reduced the activity of the surface for oxygen atom loss. It is apparent that the hydrated aluminum oxide has a lower capacity for oxygen sorption or a reduced catalytic activity for atom recombination, relative to the dehydrated form. Since the precise chemical composition and crystalline form of the surfaces used in our experiments are unknown, further discussion on the mechanism of the effect of water would be purely speculative.

Changes in surface temperature over the range 140-360°K have little effect on the observed values of α for the aluminum specimens (Table 3). The total observed saturation coverage of anodized aluminum at 140°K was about twice that at 360°K (Table 5) but even if this coverage were attained within one minute (i.e., $\dot{n}_s$ initial = 5.6×10^{13} atoms/cm^2 min), the value of S_o would not exceed 4×10^{-2}. Similar considerations would apply to plain aluminum and the SiO_x surface, both of which exhibit very low saturation coverages of atomic oxygen at both temperature extremes. Gold, on the contrary, shows a substantial diminution in α when the temperature is reduced to 140°K, but in all likelihood would possess a value of S_o near unity at this temperature. This can be attributed to the low value of k_3 which appears to be the atom loss rate limiting process when the oxygen surface coverage is near unity. On a nearly clean surface, however, the atom loss rate is determined mainly by the adsorption step which is very rapid. The difference in the values of α at the two temperature extremes suggests an activation energy for the gasatom-surface atom recombination process (k_3) of less than 1 kcal/mole.

Additional evidence for the great disparity in atom loss rate between a clean and an oxygen-saturated surface of gold relative to that

of the other surfaces examined is found in observations of Q/Q^* under nonsteady-state conditions. The adsorption curves (Figures 5, 7, 9) indicate that 5 to 10 minutes are required to approach saturation coverage on any of the surfaces. Consequently measured values of Q/Q^* taken in the interval 0 to 5 minutes following cleaning of the surface would be expected to be less than those observed at steady state, if the atom loss rate on the sparsely covered surface exceeds that on the saturated surface. The data in Table 6 indicate this to be the case for gold, but not for the other surfaces.

It should be noted that the value of S_o for gold reported here exceeds that reported in our earlier work (ref. 3) by a factor of approximately 6. This difference resulted from a reexamination of the earlier results in the light of our new data. The method employed to estimate P_o described in this report gives a value of this parameter approximately one-third that originally estimated for the earlier work. Also, an examination of the method of atomic oxygen exposure of the specimen following heating used in the earlier experiments leads to the conclusion that the actual time of exposure was approximately 0.5 minute shorter than originally indicated. Translation of the data points by 0.5 minute on the time coordinate gives an initial slope greater by a factor of two than the original interpretation, The data from this experiment are included in Figure 5 (solid circles).

The use of the atomic oxygen-surface kinetic data in assessing the performance of the investigated materials in the Dual Air Density Satellites is discussed in a Special Technical Report issued on 13 January 1972. This report, with improved values of rate constants inserted, is reproduced in full as Appendix B.

Page Intentionally Left Blank

CONCLUSION

Plain aluminum and anodized aluminum surfaces exhibit low activity for atomic oxygen loss ($\alpha < 10^{-2}$) over the temperature range 140-360°K but show some variability, which seems to be related to the degree of hydration of the aluminum oxide surface layer. The initial sticking probability of oxygen atoms on these materials is also quite low ($S_o < 10^{-2}$).

SiO_x-coated aluminum demonstrates extremely low atom loss activity ($\alpha \leqslant 10^{-3}$) in addition to a low sticking probability ($S_o < 10^{-3}$).

Gold has a much higher atom loss activity ($\alpha > 10^{-2}$) than aluminum and an initial sticking probability which lies between 0.25 and unity in the temperature range 360-140°K.

Page Intentionally Left Blank

REFERENCES

1. U. von Zahn, J. Geophys. Res. 72, 5933 (1967), (a critical review).

2. B. R. Baker and B. J. Wood, J. Vac. Sci. Technol. 8, 555 (1971).

3. B. J. Wood, J. Phys. Chem. 75, 2186 (1971).

4. A. Guthrie and R. K. Wakerling, "Vacuum Equipment and Techniques," New York, McGraw-Hill Book Co., 1949, 35 ff. W. Steckelmacher, Vacuum 16, 561 (1966).

5. P. O. Schissel and O. C. Trulson, J. Chem. Phys. 43, 737 (1965).

6. A. S. Berman, J. Appl. Phys. 36, 3356 (1965).

7. H. Wise and B. J. Wood, Adv. Atomic Mol. Phys. 3, 296 (1967).

8. L. J. Kieffer and G. H. Dunn, Rev. Mod. Phys. 38, 1, (1966).

Page Intentionally Left Blank

Table 1

GEOMETRIC CONSTANTS OF APPARATUS

Part	Apparatus "a"			Apparatus "b"		
	Length cm	Diam cm	Conductance ℓ/sec	Length cm	Diam cm	Conductance ℓ/sec
Gas inlet	14	1.45	2.2	14	1.45	2.2
Atom source chamber	7.5	3.4	38	7.8	4.1	60
Reactor inlet	0.3	0.6	2.2	0.2	0.6	2.5
Reactor	12	2.2	8.0	12.7	3.4	26
Reactor outlet	0.3	1.1	10	0.2	1.2	12
Net conductance between pressure gages			0.87			1.0
Collision number[a], σ (based on 22 cm^2 specimen)	206			177		
Tungsten ribbon atom source	4.0 x 0.6 x 0.0025 cm					

a. $\sigma = A_s/(A_i+A_e)$. Values used for A_i and A_e were the areas of thin-edge apertures which would exhibit the conductances shown in the table (computed from the short pipe formula[4]).

Table 2

SURVIVAL OF ATOMIC OXYGEN IN EMPTY REACTOR

Reactor (Fig.1)	Transmission Probability[a]	Tungsten Ribbon Temp (°K)	P_{O_2} (calculated)[b] in atom source chamber (torr)	Q_O at Reactor Outlet (torr ℓ/sec) x 10^7	
				Observed	Predicted from data in Ref. 5
a	0.175	2170	7.1×10^{-7}	0.99	0.45
			4.1×10^{-6}	3.3	1.3
			8.2×10^{-6}	5.1	2.0
			2.7×10^{-5}	14	4.1
			5.5×10^{-5}	27	6.6
b	0.239	2250	6.1×10^{-7}	0.63	0.57
			2.6×10^{-6}	1.3	1.6
			6.4×10^{-6}	3.8	2.9
			1.5×10^{-5}	6.4	5.4
			3.1×10^{-5}	9.0	9.1

[a] Reference 6.

[b] $P_{O_2 \text{ source}} = (Q_{O_2}/F) + P_A$ where $1/F = 1/F_e + 1/F_R + 1/F_i$.

Table 3

SUMMARY OF ATOM LOSS RATE DATA

Surface	Temp[d] (°K)	Pretreatment (see text)	Q_o/Q^*_o	α_{max}[a] x10^3	α_{mean} x10^3
Plain Al 6	330	None	1.34±0.48	0.74	0
	330	Bakeout	0.98±0.16	1.1	0.1
	330	None	1.32±0.23	0	0
	330	Vac anneal	1.05±0.20	0.80	0
	330	Heated in O+O_2	0.81±0.10	1.8	1.2
Plain Al 16	330	None	1.09±0.37	1.8	0
	330	Heated in O+O_2	0.54±0.16	7.3	3.9
	360	Vac anneal	0.94±0.085	0.9	0.4
	140	Vac anneal	0.88±0.087	1.4	0.7
Anodized Al 16	330	None	1.02±0.18	0.9	0
	330	Heated in O+O_2	0.56±0.16	6.7	3.5
	330	Heated in O+O_2	0.48±0.049	6.0	5.0
	330	H_2O exposure[b]	0.80±0.16	2.5	1.2
	330	Addl. H_2O exposure[c]	0.88±0.18	1.9	0.6
	330	Vac anneal	0.70±0.087	2.0	1.9
	360	Bakeout	0.53±0.28	17	4.8
	360	None	0.75±0.24	5.1	1.8
	140	None	0.54±0.15	8.4	4.8
	360	In vac. 19 days	0.70±0.16	4.6	2.3
	360	Heated in O+O_2·50°C	0.38±0.067	12	8.8
Au-clad Al 14	360	None	0.83±0.13	1.9	1.4
	360	Heated in O+O_2	0.51±0.25	13	4.9
SiO_x clad Al 16	360	None	0.98±0.14	1.0	0.1
	360	Heated in O+O_2	1.18±0.22	0.22	0
	140	Heated in O+O_2	0.99±0.19	1.3	0.1
Gold foil	360	Vac anneal	0.47±0.14	11.	3.0
	140	Vac anneal	0.97±0.25	2.1	0.1
	330	Vac anneal	0.21	20.	20

[a] Computed from statistically lowest value of Q/Q^*.

[b] Exposure: 1.6×10^{-3} torr·min.

[c] Exposure: 0.2 torr·min.

[d] Temperature: 330°K corresponds to apparatus "a"; 360°K and 140°K correspond to apparatus "b".

Table 4

SUMMARY OF RATE CONSTANTS

Surface	Specimen Temp. °K	S_o (Eq. 6)	k_1[e] $(atoms/cm^3)^{-1}\ min^{-1}$	k_2 $(atoms/cm^2)^{-1}\ min^{-1}$	k_3 $(atoms/cm^3)^{-1}\ min^{-1}$	k_α (Eq.7)[a] $(atoms/cm^3)^{-1}\ min^{-1}$
Gold	330[c]	0.25	2.2×10^{-10}	1.5×10^{-17}	1.5×10^{-11}	1.9×10^{-11}
	360	0.30[d]	2.5×10^{-10}	(1.5×10^{-17})[b]	1.6×10^{-10}	1.6×10^{-11}
	140	1.0	--	--	--	1.9×10^{-12}
Plain Al	330[c]	4.2×10^{-3}	4.0×10^{-12}	1.8×10^{-15}	1.6×10^{-10}	6.8×10^{-11}
	360	4.6×10^{-3}[d]	---	--	--	1.3×10^{-10}
	140	2.6×10^{-2}[d]	--	--	--	3.6×10^{-11}
Anodized Al	330[c]	6.7×10^{-3}	6.4×10^{-12}	1.9×10^{-16}	1.9×10^{-10}	1.5×10^{-10}
	360	6.0×10^{-3}	5.7×10^{-12}	1.9×10^{-16}	2.9×10^{-10}	2.2×10^{-10}
	360	3.5×10^{-3}	3.3×10^{-12}	(1.9×10^{-16})	3.3×10^{-10}	4.3×10^{-10}
	140	4×10^{-2}[d]	--	--	--	1.4×10^{-10}
SiO_x on Al	360	2×10^{-4}[d]	--	--	--	7.0×10^{-10}
	140	1×10^{-3}[d]	--	--	--	3.4×10^{-9}

[a] Based on values of α_{max}, Table 3, and observed n_s at steady state.

[b] Values in parenthesis were not measured in indicated experiment but were used to compute k_3.

[c] Estimated value.

[d] Based on assumption that surface reached observed saturation coverage in 1 minute of exposure to $n_{g\ average} = 1.5\times10^{9}\ atoms/cm^3$. This would represent an upper limit value for S_o.

[e] Adsorption rate constant $k_1 = S_o v_g/4n_{s\ max}$. Values computed on basis $n_{s\ max} = 1.1\times10^{15}\ atoms/cm^2$.

Table 5

OBSERVED SATURATION COVERAGES OF OXYGEN ATOMS

($n_{g\ max} \cong 6 \times 10^{9}$ atoms/cm^{3})

Surface	n_s (atoms/cm^2) x 10^{-15}		
	T=360°K	T=330°K[a]	T=140°K
Gold	0.65	1.0	1.0
Plain Al	0.0065	0.025	0.037
Anodized Al	0.039	0.052	0.056
SiO_x on Al	0.0003		0.0004

[a]Estimated temperature.

Table 6

STEADY-STATE AND NONSTEADY-STATE VALUES OF Q/Q^*

Surface	Time interval from initial exposure of clean surface to atomic oxygen (min)	Q/Q^* observed at indicated time	Q/Q^* observed at steady state (average values)
Gold	4	0.17	0.47 ± 0.14
Gold on Al	2	0	0.51 ± 0.25
Plain Al	2	0.82	0.81 ± 0.10
	3	0.69	
Anodized al	2	0.18	0.56 ± 0.16
	2.5	0.63	
SiO_x on Al	4	0.95	1.2 ± 0.22

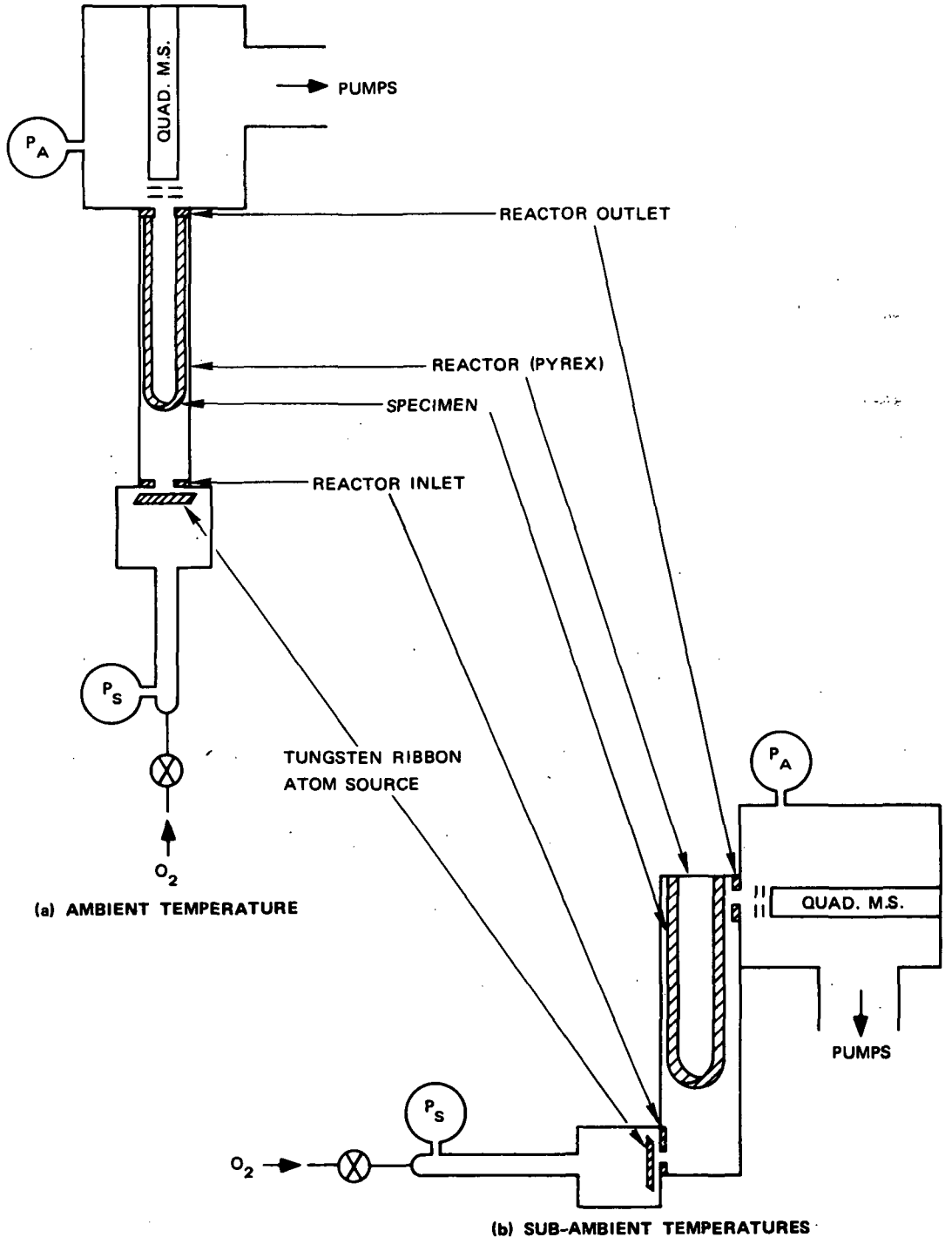

FIGURE 1 SCHEMATIC DIAGRAMS OF APPARATUS FOR EXPERIMENTS

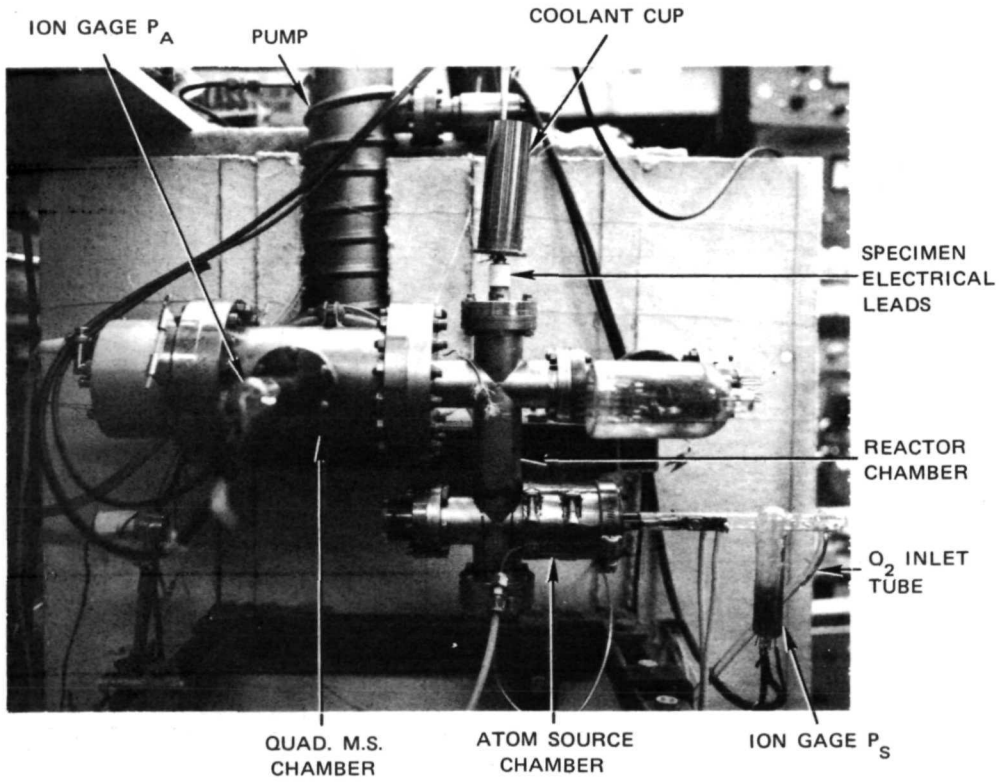

FIGURE 2 PHOTOGRAPH OF APPARATUS FOR SUB AMBIENT TEMPERATURES (FIGURE 1B)

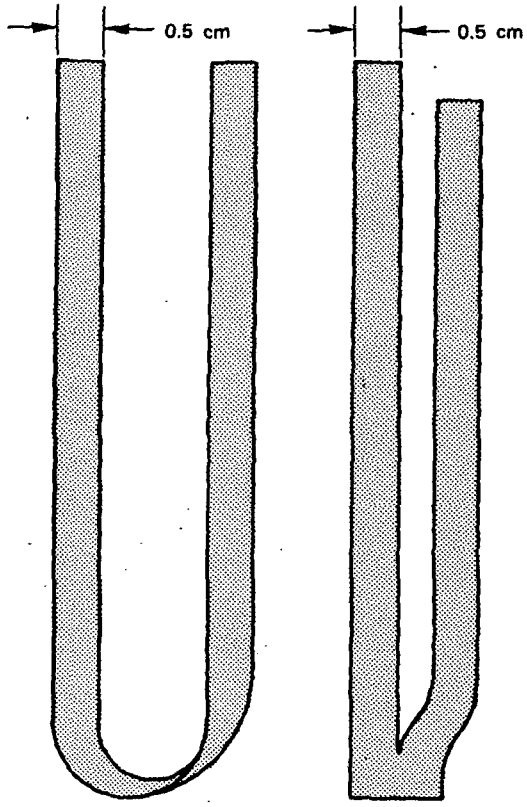

FIGURE 3 SPECIMEN CONFIGURATIONS. The foil strips were approximately 22 cm in total length. The geometric surface area was 22 cm^2.

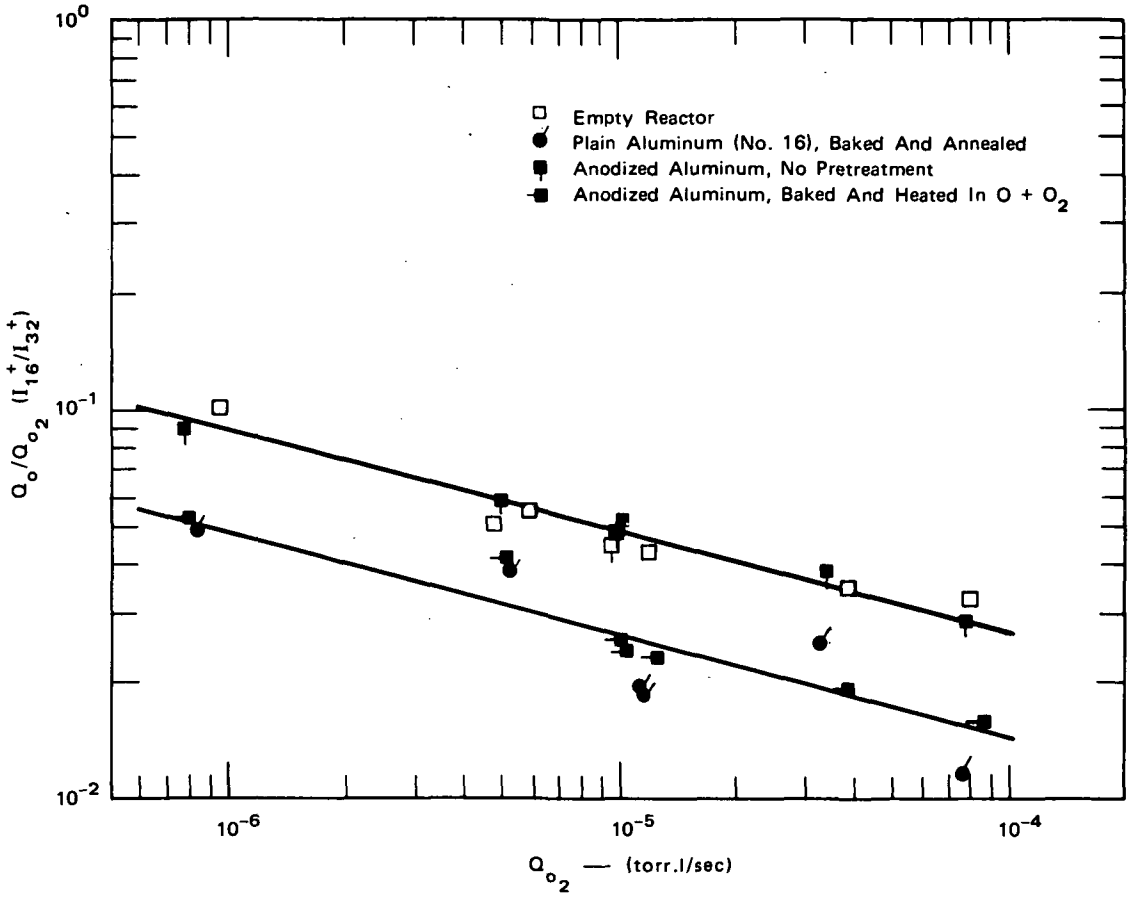

FIGURE 4 TYPICAL EXPERIMENTAL DATA. T = 330°K

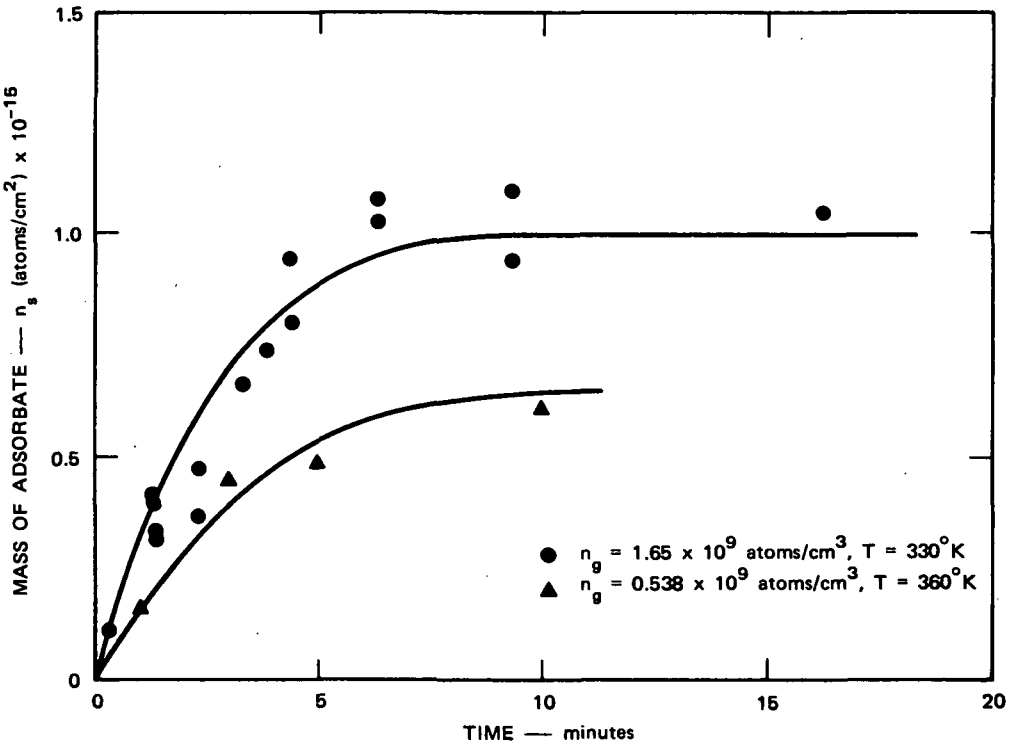

FIGURE 5 ADSORPTION OF ATOMIC OXYGEN ON GOLD FOIL

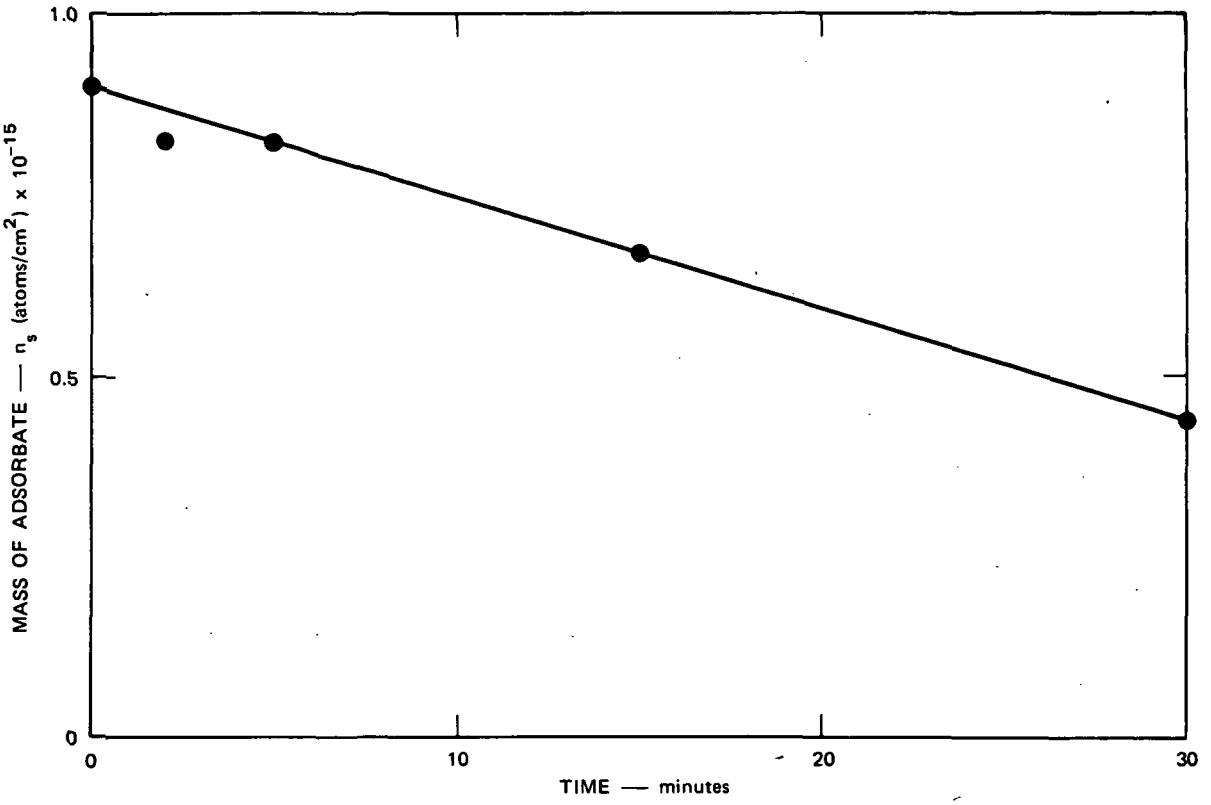

FIGURE 6 DESORPTION OF OXYGEN FROM GOLD. n_g = 0. T = 330°K.

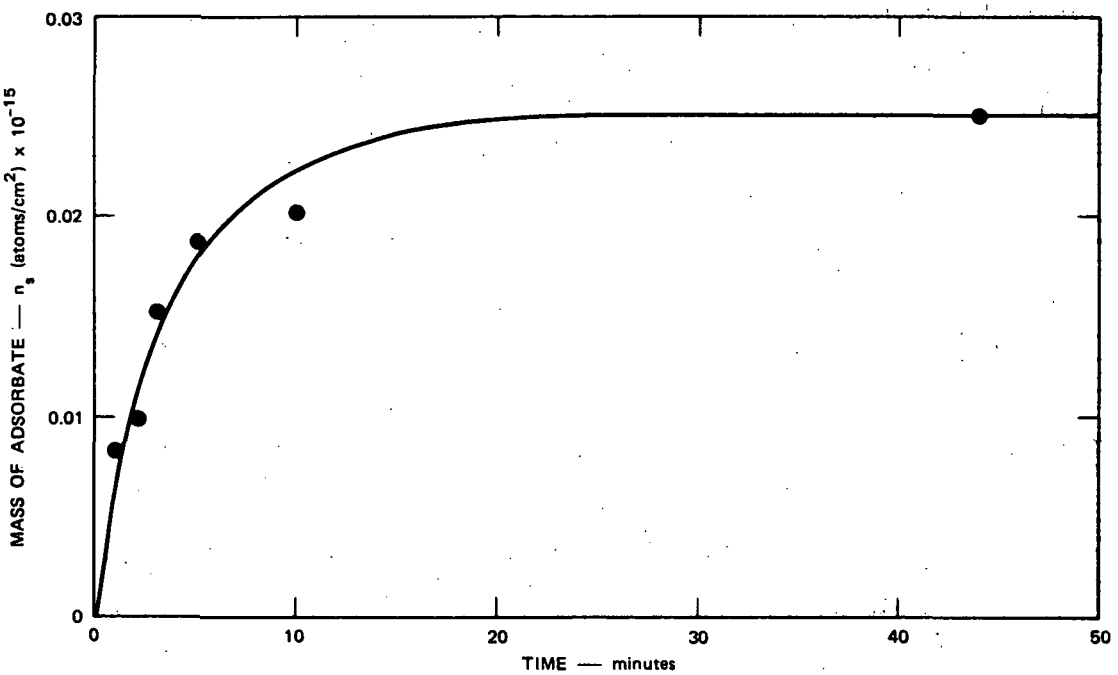

FIGURE 7 ADSORPTION OF ATOMIC OXYGEN ON PLAIN ALUMINUM (SPECIMEN NO. 6). n_g = 1.5 x 10^9 atoms/cm^3. T = 330°K.

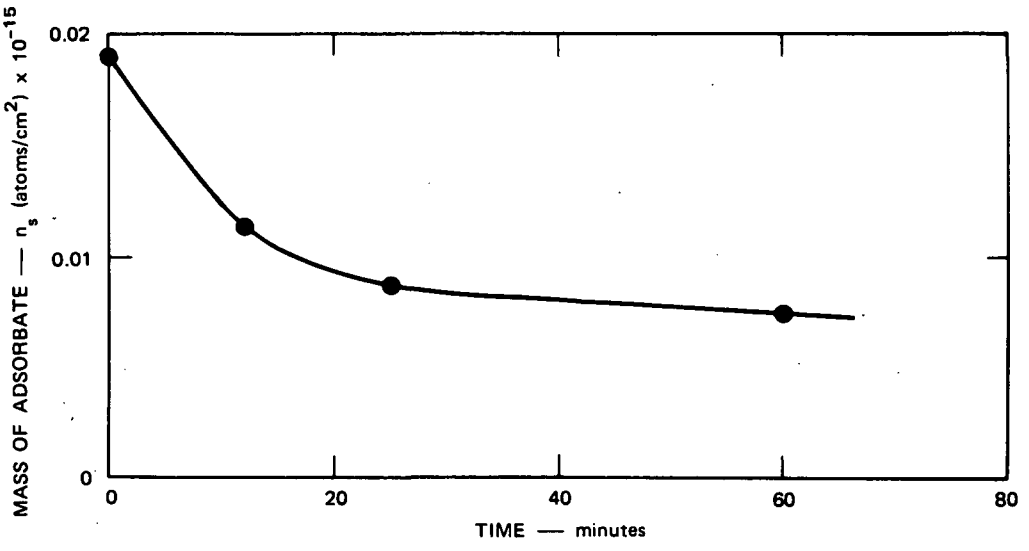

FIGURE 8 DESORPTION OF OXYGEN FROM PLAIN ALUMINUM. n_g = 0. T = 330°K.

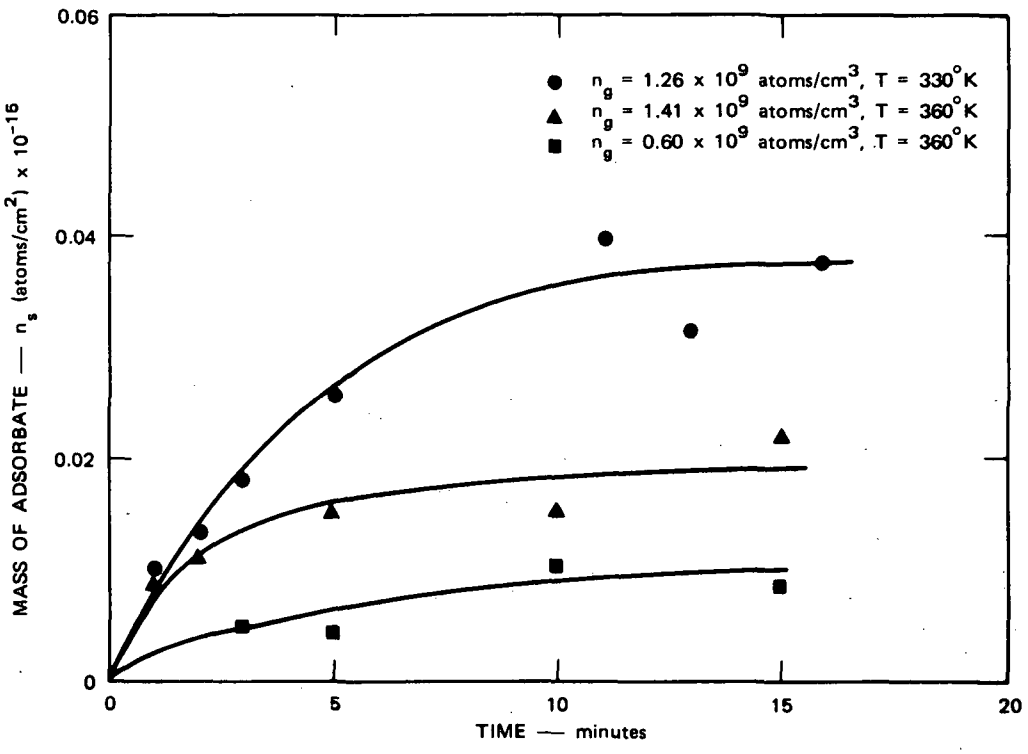

FIGURE 9 ADSORPTION OF ATOMIC OXYGEN ON ANODIZED ALUMINUM

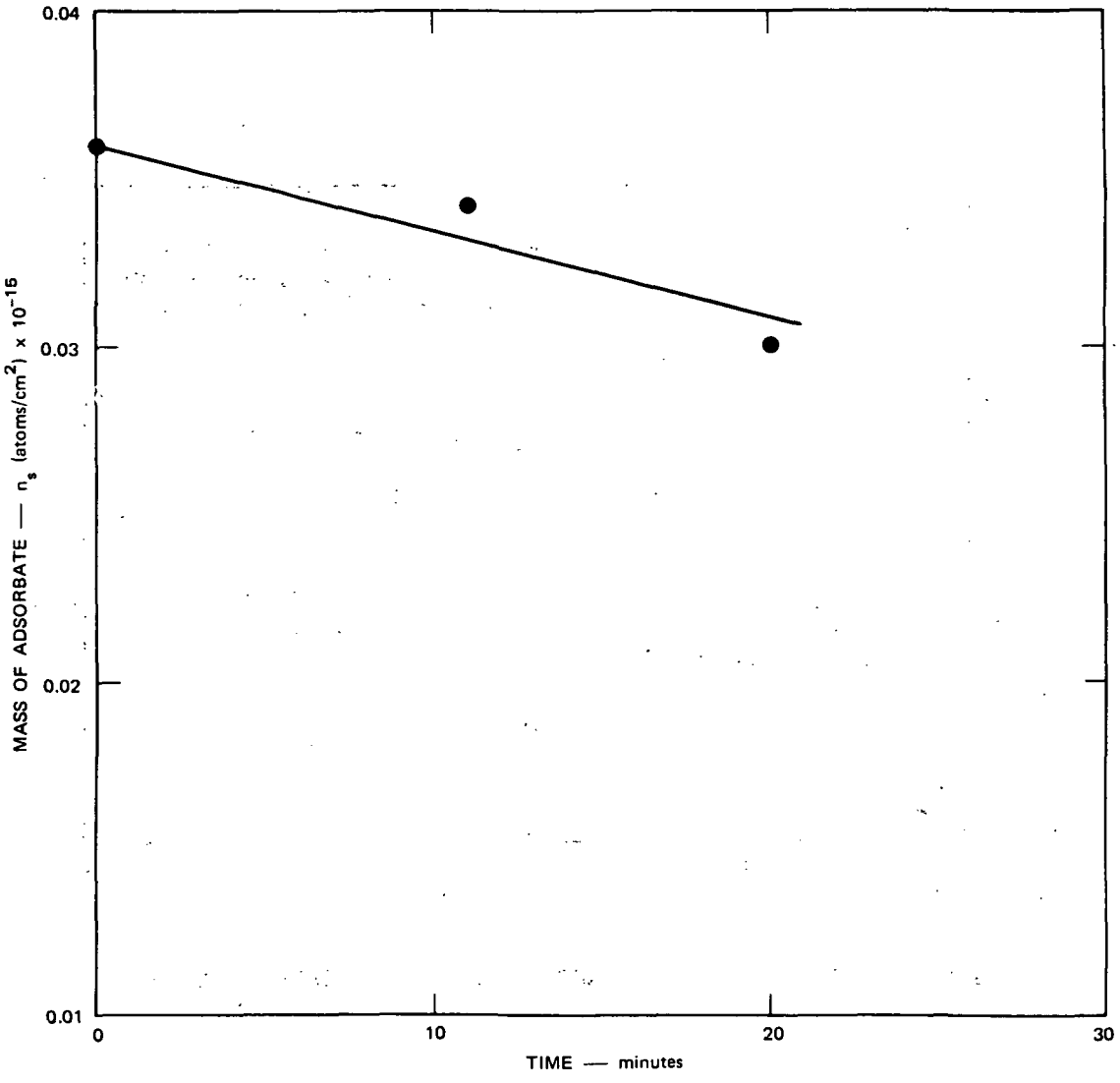

FIGURE 10 DESORPTION OF OXYGEN FROM ANODIZED ALUMINUM. n_g = 0. T = 330°K.

APPENDIX A

DETERMINATION OF ATOMIC OXYGEN FROM OBSERVED ION CURRENTS

The intensity of any peak in a mass spectrum represents the sum of contributions of all substance which give fragments at that mass number. Thus

$$I_h^+ = H\Sigma P_n m_{h,n}$$

where I_h^+ is the ion current at AMU h, P is the pressure of component n, m is the fraction of component n appearing at AMU h (the cracking factor), and H is the pressure calibration coefficient for the mass spectrometer, assumed to be identical for each component. For the case of atomic oxygen (h=16), components which appear at AMU 18 (H_2O), AMU 28 (CO), AMU 32 (O_2) and AMU 44 (CO_2) contribute significantly to I_{16}^+. The cracking factors for these substances, determined in our apparatus with a fixed ionizing current (0.5 ma) and electron energy (50 v), are tabulated below:

$$m_{16,16} = 1$$
$$m_{16,18} = 0.023$$
$$m_{16,28} = 0.013$$
$$m_{16,32} = 0.112$$
$$m_{16,44} = 0.048$$
$$m_{28,44} = 0.128$$

These values are precise to within ±10%. In the case of $m_{16,32}$, a 10% variation represents an unacceptably large uncertainty in the correction. Consequently, this cracking factor was re-evaluated with each experiment over a broad range of oxygen pressures, to attain a precision of ±3%.

A set of simultaneous equations may thus be written for the components of interest:

$$I_{16}^{+} = H\left[P_O \cdot 1 + P_{H_2O} \cdot m_{16,18} + P_{CO} \cdot m_{16,28} + P_{O_2} \cdot m_{16,32} + P_{CO_2} \cdot m_{16,44}\right]$$

$$I_{18}^{+} = HP_{H_2O}$$

$$I_{28}^{+} = H\left[P_{CO} \cdot 1 + P_{CO_2} \cdot m_{28,44}\right]$$

$$I_{32}^{+} = HP_{O_2}$$

$$I_{44}^{+} = HP_{CO_2}$$

Solving these equations for the corrected value of ion current at AMU 16 (that fraction of the observed ion current contributed by atomic oxygen) we obtain:

$$HP_O = I_{16}^{+} - 0.023I_{18}^{+} - 0.013I_{28}^{+} - 0.112I_{32}^{+} - 0.046I_{44}^{+} \quad .$$

APPENDIX B

ATOMIC OXYGEN SAMPLING BY A SPHERICAL SATELLITE-- A MATHEMATICAL MODEL

Introduction

The basic objective of this project is to evaluate the kinetics and mechanism of surface interaction of oxygen atoms with candidate materials for the Dual Air Density Explorer Satellites. We have obtained room-temperature data for plain and anodized aluminum and for gold, which provide considerable insight into the mechanism of atomic oxygen reactions at the surfaces of these metals. These results have been reported in our regular monthly progress letters.

There is a need, however, to translate our kinetic data to the dynamic situation of the satellites themselves. To meet this need, we have carried out a direct analysis which includes surface chemical kinetics in addition to gas dynamics for the orbiting satellites. This analysis is of immediate interest, yet it is separate from our principal experimental work. Hence, we shall describe and discuss it in this Special Technical Report.

Statement of the Problem

The Dual Air Density Explorer Satellites will be constructed as hollow spheres with uniformly perforated surfaces. Ambient gaseous oxygen atoms will enter the spheres through these perforations. Once inside, the atoms may adsorb and recombine on the interior surface. It will be important to know the relationship between the ambient atom number density and the atom number density within the sphere. Consequently, we have formulated for this purpose a mathematical model of such a spherical satellite.

The model is based on a dynamic balance between the rate of influx of atoms and the rate of atom loss by surface adsorption and reaction. Numerical calculations, using values of reaction rate constants and sticking coefficients evaluated in our laboratory experiments, provide a basis for predicting the performance of aluminum and of gold as surface materials. Since data on the temperature coefficient of the different surface processes are not yet available, the effect of surface temperature variation could not be included in the current analysis.

The Model

A hollow spherical satellite of radius R(cm), whose surface has hole fraction h, has concentration n(atoms/cm^3) of oxygen atoms in its interior and concentration n_s(atoms/cm^2) on its inner surface while passing through an atmosphere with concentration n_A (atoms/cm^3). The free atom speed is v_g(cm/sec) and satellite speed v(cm/sec). Conservation equations for volume and surface atoms read

$$\frac{4}{3}\pi R^3 \frac{dn}{dt} = 4\pi R^2 h(v_g/4)(n_A - n) + \pi R^2 h f v n_A$$

$$- 4\pi R^2(1 - h)\, n\, [S_o(v_g/4)(1 - n_s/n_{s\ max}) + k_3 n_s]$$

$$4\pi R^2(1 - h) \frac{dn_s}{dt} = 4\pi R^2(1 - h)[S_o n(v_g/4)(1 - n_s/n_{s\ max}) - k_3 n_s n - k_2 n_s^2]$$

where S_o is the fraction that stick of the $(nv_g/4)$(atoms/cm^2 sec) approaching the surface, k_2 and k_3 are rate coefficients for heterogeneous oxygen atom recombination into molecules on the surface, f is the fraction that remain of the atoms swept up by the satellite holes, and concentration $n_{s\ max}$(atoms/cm^2) is the value of n_s for a complete monolayer.

The equations are simplified by introducing θ, the fraction of surface coverage.

$$\theta = n_s/n_{s\ max}$$

$$\frac{4R}{3hv_g}\ \frac{dn}{dt} = (1 + V)\ n_A - n[1 + pS_o(1-\theta) + pK_3\theta]$$

$$\frac{4n_{s\ max}}{v_g}\ \frac{d\theta}{dt} = n[S_o(1 - \theta) - K_3\theta] - K_2\theta^2$$

where

$$p = (1 - h)/h,\ V = fv/v_g,\ K_2 = 4k_2\ n^2_{s\ max}/v_g,\ K_3 = 4k_3 n_{s\ max}/v_g$$

Solution of the Equations

The differential equations for n and θ are nonlinear and not likely to have a simple solution. The coefficient of n in the first equation is a linear function of θ which varies between $(1 + pS_o)$ and $(1 + pK_3)$ as θ varies from 0 to 1. Bounds on the unsteady solution for n are obtained if this coefficient is given one of these values.

For any fixed initial condition, the solution n_B to

$$\frac{4R}{3hv_g}\ \frac{dn_B}{dt} = (1 + V)\ n_A - n_B\ B$$

is seen to be an upper bound to true values of n if B is the smaller of its two values or a lower bound if B is the larger.

One finds

$$n_B = n_{BO}e^{-bt} + (b/B)\int_o^t (1 + V)\ n_A(\tau)\ e^{-b(t - \tau)}d\tau$$

where

$$b = 3Bhv_g/4R$$

and n_{BO} is the value of n_B at t = 0.

For a satellite, $(1 + V)n_A$ is a periodic function of time with the satellite period T. The function has a Fourier expansion

$$(1 + V)\, n_A(t) = \sum_{m=0}^{\infty} n_{Am} \cos(2\pi mt/T) \ .$$

Carrying through the integrations gives

$$n_B = n_{BO} e^{-bt}$$

$$+ (b/B) \sum n_{Am} [b \cos (2\pi mt/T) + (2\pi m/T) \sin(2\pi mt/T)]$$

$$\div [b^2 + (2\pi m/T)^2]$$

For large t the transient term is negligible. If t is an integral multiple of T one has

$$(1 + V)\, n_A = \sum n_{Am}$$

$$n_B = (b^2/B) \sum n_{Am}/[b^2 + (2\pi m/T)^2]$$

so that the higher frequency Fourier components of n_A have decreased importance for n_B and the true n.

Numerical Computations

Based on values of satellite parameters supplied by Langley Research Center, we computed the maximum and minimum values of velocities of the two satellites.

Orbit Data:

r = distance from center of earth

β = angle in orbit

a = semimajor axis of elliptical orbit

e = eccentricity of orbit ellipse

$$r = a(1 - e^2)/(1 + e \cos \beta)$$

Radius of earth = 6378 km

Period T = 108 min

$a(1 + e)$ = 7878 km (apogee value of r)

Two cases:

Upper satellite:	Lower satellite:
$a(1 - e)$ = 7078 km	$a(1 - e)$ = 6778 km (perigee)
e = 0.0535	e = 0.0751
a = 7478 km	a = 7328 km
D = 365 cm	D = 76.2 cm

h = 0.01

From $r^2\dot{\beta} = K$, a constant, find $T = \int_o^{2\pi} \frac{r^2}{K}\, d\beta$

and then

$$K = \frac{2\pi A^2}{T}\sqrt{(1 - e^2)}$$

$$v^2 = \dot{r}^2 + r^2\,\dot{\beta}^2 = [K^2/a^2(1 - e^2)^2](1 + e^2 + 2e\cos\beta)$$

$$\therefore\ v_{max} = 2\pi\,\frac{a}{T}\sqrt{\frac{1 + e}{1 - e}}$$

$$v_{min} = \frac{1 - e}{1 + e} \cdot v_{max}$$

Upper satellite:	Lower satellite:
v_{max} 456 km/min	456 km/min
v_{min} 410	396

For v_{max} = 456 km/min, v_g = 38.4 km/min, h = 0.01, and f = (1 - h), we computed the values of the constants p = 100 and V = 11.85.

Surface Interaction Data:

Values of sticking probability and surface recombination rate constants obtained from our experimental measurements together with the value $n_{s\ max} = 10^{15}$ atom/cm,^{2} were used to compute the remaining derived constants. These values are tabulated below.

	Anodized Aluminum	Gold
S_o	6.7×10^{-3}	0.30
k_2(atoms/cm^2)$^{-1}$ min^{-1}	1.9×10^{-16}	1.5×10^{-17}
k_3(atoms/cm^3)$^{-1}$ min^{-1}	1.9×10^{-10}	1.6×10^{-11}
K_2(atoms/cm^3)	2.0×10^{8}	1.6×10^{7}
K_3	0.20	0.18
B $\begin{cases} \vartheta \to 1 \\ \theta \to 0 \end{cases}$	21 1.7	19.2 31
b(min^{-1}) $\begin{cases} \text{upper} \\ \text{lower} \end{cases}$	157 B 754 B	157 B 754 B

Since

$$V = 11.85$$

$$n_{A\ min} = 0$$

$$n_{A\ max} = \begin{cases} 4.0 \times 10^5 & \text{upper} \\ 6.3 \times 10^7 & \text{lower} \end{cases}$$

one has approximately

$$(1 + V)n_A = 6.42\ n_{A\ max}[1 + \cos(2\pi/T)] = n_{AO} + n_{A1} \cos(2\pi t/T)$$

$$n_B = 6.42\ \frac{n_{Amax}}{B} \left\{1 + \frac{\cos 2\pi(t/T - \varphi)}{[1 + (2\pi/bT)^2]^{\frac{1}{2}}}\right\}$$

where $\tan \varphi = \frac{2\pi}{bT}$

Since $\frac{2\pi}{bT} \leq \frac{2\pi}{108 \times 157 \times 5.0} = 7.4 \times 10^{-5}$ in all cases, phase lag φ is negligibly small. Thus n_B and n itself are determined by the current value of n_A:

$$n_B = n_A(1 + V)/B$$

Since n lies between the two values of n_B,

$$0.20 < \frac{n}{n_A} < 7.7 \quad \text{for anodized aluminum}$$

and

$$0.42 < \frac{n}{n_A} < 0.67 \quad \text{for gold.}$$

A time scale for transients in coverage θ is

$$4\, n_{s\ max}/K_2 v_g = \begin{cases} 5 \text{ min for anodized aluminum} \\ 65 \text{ min for gold.} \end{cases}$$

Conclusions

It is found that n, the atom concentration in the sphere, is proportional to n_A, the ambient concentration. For a gold surface, the constant of proportionality is nearly independent of θ, the surface coverage. For an anodized aluminum surface, the proportionality can vary over wide limits as θ varies, so that the relation between n and n_A can be obtained only by integration of the differential equations. It is important to note, however, that if $n_{s\ max}$ has a lower value, as may well be the case for aluminum oxide, the span in values of n/n_A will be reduced.

The time scale of θ is of the order of minutes. Hence θ is nearly constant for shorter time intervals, and the fractional time rates of change of n and of n_A over short times will be equal.

"The aeronautical and space activities of the United States shall be conducted so as to contribute . . . to the expansion of human knowledge of phenomena in the atmosphere and space. The Administration shall provide for the widest practicable and appropriate dissemination of information concerning its activities and the results thereof."

—NATIONAL AERONAUTICS AND SPACE ACT OF 1958

NASA SCIENTIFIC AND TECHNICAL PUBLICATIONS

TECHNICAL REPORTS: Scientific and technical information considered important, complete, and a lasting contribution to existing knowledge.

TECHNICAL NOTES: Information less broad in scope but nevertheless of importance as a contribution to existing knowledge.

TECHNICAL MEMORANDUMS: Information receiving limited distribution because of preliminary data, security classification, or other reasons. Also includes conference proceedings with either limited or unlimited distribution.

CONTRACTOR REPORTS: Scientific and technical information generated under a NASA contract or grant and considered an important contribution to existing knowledge.

TECHNICAL TRANSLATIONS: Information published in a foreign language considered to merit NASA distribution in English.

SPECIAL PUBLICATIONS: Information derived from or of value to NASA activities. Publications include final reports of major projects, monographs, data compilations, handbooks, sourcebooks, and special bibliographies.

TECHNOLOGY UTILIZATION PUBLICATIONS: Information on technology used by NASA that may be of particular interest in commercial and other non-aerospace applications. Publications include Tech Briefs, Technology Utilization Reports and Technology Surveys.

Details on the availability of these publications may be obtained from:

SCIENTIFIC AND TECHNICAL INFORMATION OFFICE

NATIONAL AERONAUTICS AND SPACE ADMINISTRATION

Washington, D.C. 20546